

X-ray luminosities of galaxies in groups

Stephen F. Helsdon^{*1}, Trevor J. Ponman¹, Ewan O’Sullivan¹
and Duncan A. Forbes^{1,2}

¹*School of Physics and Astronomy, University of Birmingham, Edgbaston, Birmingham B15 2TT, UK*

²*Astrophysics & Supercomputing, Swinburne University of Technology, Hawthorn VIC 3122, Australia*

Accepted 2000 ??; Received 2000 ??; in original form 2000 ??

ABSTRACT

We have derived the X-ray luminosities of a sample of galaxies in groups, making careful allowance for contaminating intragroup emission. The $L_X:L_B$ and $L_X:L_{FIR}$ relations of spiral galaxies in groups appear to be indistinguishable from those in other environments, however the elliptical galaxies fall into two distinct classes. The first class is central-dominant group galaxies which are very X-ray luminous, and may be the focus of group cooling flows. All other early-type galaxies in groups belong to the second class, which populates an almost constant band of L_X/L_B over the range $9.8 < \log L_B < 11.3$. The X-ray emission from these galaxies can be explained by a superposition of discrete galactic X-ray sources together with a contribution from hot gas lost by stars, which varies a great deal from galaxy to galaxy. In the region where the optical luminosity of the non-central group galaxies overlaps with the dominant galaxies, the dominant galaxies are over an order of magnitude more luminous in X-rays.

We also compared these group galaxies with a sample of isolated early-type galaxies, and used previously published work to derive $L_X:L_B$ relations as a function of environment. The non-dominant group galaxies have mean L_X/L_B ratios very similar to that of isolated galaxies, and we see no significant correlation between L_X/L_B and environment. We suggest that previous findings of a steep $L_X:L_B$ relation for early-type galaxies result largely from the inclusion of group-dominant galaxies in samples.

Key words: galaxies: ISM – galaxies: elliptical and lenticular – galaxies: spiral – X-rays: galaxies

1 INTRODUCTION

Many galaxies in the Universe are found in galaxy groups (e.g. Tully 1987). These group galaxies show some differences from their counterparts in the field. For example, there is evidence that some spirals interact with their environment (Verdes-Montenegro et al. 2000), and with each other (e.g. Rubin et al. 1991; Forbes 1992). Early-type galaxies in groups are less likely to have boxy isophotes and more likely to have irregular isophotes than comparable ellipticals in other environments (Zepf & Whitmore 1993). Many of these features are likely to be due to the effects of the group environment in which the galaxy is found, and it is possible that the X-ray properties of galaxies could be affected by the group environment as well.

There are two main sources for the X-ray emission from normal galaxies: stellar sources and hot diffuse interstel-

lar gas. Emission from bright early-type galaxies is dominated by the hot diffuse component (e.g. Forman et al. 1985; Trinchieri & Fabbiano 1985) whilst in late-type and less luminous early types, the emission is primarily from stellar sources (e.g. Fabbiano & Trinchieri 1985; Kim et al. 1992). There have been a number of studies of the X-ray properties of both spiral (e.g. Fabbiano & Trinchieri 1985; Fabbiano et al. 1988) and elliptical (e.g. Canizares et al. 1987; Eskridge et al. 1995; Brown & Bregman 1998; Beuing et al. 1999) galaxies, which show that while the X-ray luminosity of late-type galaxies scales roughly with the optical luminosity, the same relation for early-type galaxies is considerably steeper and shows much more scatter.

If environment does have a significant effect on galaxy X-ray properties, this could explain some of the scatter observed in the $L_X:L_B$ relations for galaxies. A galaxy moving through the intragroup medium may undergo ram pressure stripping (Gunn & Gott 1972) or viscous stripping (Nulsen 1982), thus decreasing the X-ray luminosity with-

* E-mail: sfh@star.sr.bham.ac.uk

out much affecting the stellar luminosity. Conversely, material cooling onto a galaxy from the intragroup medium could enhance the observed galaxy X-ray luminosity (Canizares et al. 1983). The effects of galaxy winds may also play an important role. Brown & Bregman (2000) found a positive correlation between L_X/L_B and local galaxy volume density, for early-type galaxies using *ROSAT* data. They suggested that the X-ray luminosity of early-type galaxies is enhanced in higher density environments. This is in contrast to the earlier work of White & Sarazin (1991) who claimed detection of the opposite effect, using *Einstein* data.

In practice, study of the X-ray properties of galaxies within groups is complicated by the presence of X-ray emission from a hot intragroup medium in many bound groups (Mulchaey et al. 1996; Ponman et al. 1996; Helsdon & Ponman 2000). Many previous studies of the X-ray emission from galaxies, especially early-type galaxies, which predominate in X-ray bright groups, have failed to allow for this problem. This can result in poor estimates for the luminosity, extent and spectral properties of galaxy emission. In the present paper we attempt to remedy this by carefully removing group emission, which in some cases involves using multicomponent models of the surface brightness distribution (Helsdon & Ponman 2000) within a group. By comparing the properties of these galaxies to those in low density environments we seek to gain some insight into the processes operating in the group environment. Throughout this paper we use $H_0=50 \text{ km s}^{-1} \text{ Mpc}^{-1}$, and all errors are 1σ .

2 A SAMPLE OF GROUP GALAXIES

In order to investigate the X-ray properties of galaxies in groups, it is first necessary to define a sample of groups with available X-ray data. For this study we have combined the sample of groups studied by Helsdon & Ponman (2000) with additional data for compact galaxy groups. We use only galaxies from groups in which a hot intragroup medium is detected, since this confirms that these groups are genuine mass concentrations, as opposed to chance line-of-sight superpositions.

Helsdon & Ponman (2000) compiled a sample of 24 X-ray bright groups observed with the *ROSAT* PSPC. In the case of compact galaxy groups, the tight configuration of the major group galaxies (typically separated by only a few arcminutes) can lead to serious problems of confusion, and contamination of galaxy fluxes by diffuse group emission. We therefore have added to the sample all the Hickson Compact Group (HCG; Hickson 1982) galaxies observed by the *ROSAT* HRI. The HCGs thus added were 15, 16, 31, 44, 48, 51, 62, 68, 90, 91, 92, and 97. In the case of overlap between the HRI data and the PSPC data of Helsdon & Ponman (2000) (HCGs 62, 68 and 90), the HRI data were preferentially used, except in the case of HCG 62. In the case of HCG 62, the diffuse group emission is so bright that no galaxies could be detected, and upper limits were dominated by uncertain systematic errors in modeling the diffuse flux. However the PSPC data for this system clearly show a central component, fairly distinct from the surrounding group emission; a structure very similar to that of a number of other PSPC groups. We have therefore omitted this group from the HRI dataset and used the PSPC data instead. This

resulted in a final sample of 33 groups, 11 HCGs with HRI data and 22 other groups with PSPC data. Note that the PSPC data contains two compact groups (HCG 42 & HCG 62), which are listed under the names given in Helsdon & Ponman (2000) (NGC 3091 & NGC 4761).

Principal galaxies in the HCGs are listed with types and magnitudes in Hickson et al. (1989). The sample for which we were able to derive useful X-ray flux estimates or upper limits, contains 46 galaxies in 11 HCGs. For the loose groups, we wished to include only galaxies residing within the denser inner regions, where environmental effects might be expected. We therefore searched the NASA/IPAC Extragalactic Database (NED) for galaxies lying within a third of the group virial radius in projection on the sky, and having recession velocities within three times the group velocity dispersion ($3\sigma_g$) of the catalogued group mean. The virial radius of each group (typically ~ 1.1 Mpc) is calculated as described in Helsdon & Ponman (2000), which also lists σ_g for each group. All galaxies with a listed optical magnitude and galaxy type were initially included. A number of extra galaxies were included with galaxy types from Zabludoff & Mulchaey (1998), who have carried out multi-fibre spectroscopy on 9 of the groups. Also included were a few galaxies whose galaxy types were easily determined from Digitized Sky Survey images. This gave a total of 114 galaxies (in 22 loose groups) for which we were able to derive useful X-ray flux estimates or upper limits. These were split into four broad morphological categories i.e. spiral, elliptical, lenticular and irregular. Adding the HCG galaxies gives a total sample of 160 galaxies in 33 groups. This sample should not be regarded as being statistically complete in any way, but rather a reasonably representative sample of galaxies in collapsed groups.

3 DATA REDUCTION

3.1 ROSAT HRI data

HRI data were reduced using standard ASTERIX software, and binned into $3''$ pixel images, using the full energy range of the detector. Due to the compact nature of HCGs, almost all galaxies studied lie within $5'$ of the pointing axis, so that vignetting affects their detected fluxes by $< 3\%$, and no correction was applied for this.

The high resolution of the HRI generally provides a clear separation between the galaxy and group emission, and in many cases the latter was undetectable. Radial profiles centred on each galaxy were used to determine the radial extent of galaxy-related emission, and the galaxy count rate was then extracted from a circle encompassing this emission. In most cases the background was flat, and was determined from a large source-free region near the centre of the field. A few systems with bright diffuse X-ray emission were more difficult. Wherever diffuse group emission might contribute more than 5% contamination to the galaxy fluxes (i.e. HCG 51, 90 and 97), we fitted an elliptical model to the diffuse flux distribution, and this was then used as a background model when deriving galaxy count rates or upper limits. In the case of HCG 92, the diffuse emission is very irregular, since it apparently arises from intergalactic shocks, rather than a hydrostatic intragroup medium (Pietsch et al. 1997).

Since we were unable to reliably model this emission, three of the five galaxies in this system had to be excluded from our sample.

Source count rates, together with Poisson errors were extracted and background subtracted. Cases where the source counts exceeded twice the Poisson error on the background (σ_b) were deemed to be detections. For non-detected sources, an upper limit of $3\sigma_b$ is returned, normally calculated within a circle of radius $18''$. All count rates were converted to unabsorbed bolometric luminosities assuming a 1 keV Raymond & Smith (1977) model with 0.25 solar metallicity, and distances given in Table 1. This model was selected as it should provide a reasonable description of the spectral properties of an early-type galaxy (Davis & White 1996). For the spiral and irregular galaxies a hotter spectral model may be more appropriate, but for simplicity the same spectral model was used for all galaxies. If a hotter temperature of 5 keV is used instead, the luminosities of the late-type galaxies would rise by about 0.24 dex. B-band luminosities were derived using magnitudes from NED, and assuming a solar blue luminosity of 5.41×10^{32} erg s⁻¹.

3.2 ROSAT PSPC data

Previous work on the X-ray properties of galaxies tends to use one of two approaches: (a) trace the extent of the emission from the galaxy position out to a background level, and include all this emission as the galaxy emission (e.g. Beuing et al. 1999), or (b) extract the emission within some standard radius, such as four times the optical effective radius of the galaxy (e.g. Brown & Bregman 1998). The first method may significantly overestimate the X-ray luminosity of any galaxy located near the centre of a group, while the second takes no account of the X-ray surface brightness profile of the galaxy, and so could result in an over- or underestimate of the true luminosity.

For the galaxies in loose groups, we adopted one of two different methods to derive X-ray luminosities, depending on their position within the group, as described in sections 3.2.1 and 3.2.2 below. 2-dimensional models of the group emission were available for each of the 22 loose groups (Helsdon & Ponman 2000). For a number of systems, these model fits indicated the presence of a central cusp, in addition to more extended emission associated with the group as a whole. Such central components invariably coincide with a central galaxy. For these cases we take the central component to be the emission associated with the galaxy. For these and all the other galaxies we are able to use the group models to remove the group contribution to the galaxy flux. In the case of HCG 62, the central X-ray component is centred on the brightest galaxy, HCG 62a, but also encompasses a second galaxy (HCG 62b). We identify this X-ray component with HCG 62a, but inclusion of the second galaxy would only reduce the derived L_X/L_B by 50% (-0.18 in $\log(L_X/L_B)$).

For the remainder of this paper, galaxies coincident with clear central X-ray cusps will be referred to as central-dominant galaxies. The brightest group galaxy (BGG) refers to the optically brightest member. It should be noted that a central-dominant group galaxy will generally be a BGG, although a BGG will not necessarily be a central-dominant galaxy as defined here.

3.2.1 Central-dominant galaxies

For 11 of the groups, Helsdon & Ponman (2000) have derived two-component fits, involving an extended group component and a central component coincident with a central, optically bright galaxy. In a few of these cases the central component was poorly resolved by the ROSAT PSPC so we examined HRI data if available, in order to check the properties of the central components. These checks showed that use of the HRI data did not significantly alter the properties of the central components derived by the PSPC. Thus for these 11 cases we have used the central component from the PSPC fits to derive the luminosity associated with the central galaxy. We have also added to these 11, the group NGC 4325, for which we have fitted a 2 component model. Helsdon & Ponman (2000) found that a one component model was adequate for this system, however the addition of a second component does significantly improve the fit ($\Delta\text{Cash} = 43.6$). The luminosity for each of these 12 cases was derived by using the 2D models to calculate the fraction of the total luminosity of the group emission contained in the central component. This contribution was then extracted from the group total luminosity given in Helsdon & Ponman (2000) to give the luminosity of the galaxy itself.

3.2.2 Other group galaxies

Initial reduction of the ROSAT PSPC data was carried out as in Helsdon & Ponman (2000). An image of the group was then generated and a radial profile produced for each galaxy listed in Table 1. These profiles were examined individually and used to identify the radius to which emission could be traced. In cases where poor statistics prevented extraction of a reliable profile, a fixed radius of 20 kpc was used. Examination of both the image and radial profiles also enabled the identification of cases where the X-ray data may be contaminated by a nearby bright source, possible cases of source overlap or cases where the galaxies may be partially obscured by the PSPC support ring. Such cases (20 galaxies in total) were excluded from further analysis. Of these 20 galaxies, 8 were removed due to the PSPC ring and the majority of the remainder were galaxies probably confused with a central galaxy X-ray component. In almost all these confused cases the central galaxy was much brighter than the removed galaxy. Even if all the optical light from these other galaxies was included, the derived L_X/L_B of the affected central galaxy would typically only change by 5% (0.02 in log space. HCG 62a, discussed earlier, is the case with the largest change).

For each galaxy, a count rate was extracted within the radius as determined above, and then corrected to an on-axis count rate. As all these galaxies lie within X-ray bright groups, a fraction of the count rate will be due to group emission. To correct for this, the best fitting 2D surface brightness profile models derived by Helsdon & Ponman (2000) were used to determine the contribution from the group, which was then subtracted from the count rate extracted at the position of the galaxy.

Detections and upper limits were derived, and converted to source luminosities (bolometric), in the way described above for compact group galaxies. The luminosities of all the group galaxies in our sample are listed in Table 1.

Galaxy name	Type	L_B	L_X	Galaxy name	Type	L_B	L_X
NGC 315 group 96 Mpc				NGC 4065 group 151 Mpc			
NGC 315	E	11.27	<41.09	NGC 4065	E	11.11	41.44 ± 0.30
NGC 311	S0	10.55	40.46 ± 0.22	NGC 4061	E	10.90	41.28 ± 0.12
NGC 383 group 102 Mpc				NGC 4072	S0	10.30	<40.88
NGC 383	S0	10.95	42.30 ± 0.06	NGC 4060	S0	10.30	<40.82
NGC 386	E	10.07	40.29 ± 0.28	NGC 4066	E	10.96	$41.94 \pm .07$
NGC 380	E	10.76	$41.58 \pm .04$	PGC 038163	S	10.18	<40.84
NGC 385	S0	10.63	$41.16 \pm .08$	NGC 4074	S0	10.38	41.37 ± 0.14
UGC679	S	9.56	<40.440	NGC 4076	S	10.80	<40.80
NGC 375	E	9.91	40.77 ± 0.18	NGC 4070	E	10.89	40.96 ± 0.31
NGC 384	E	10.58	$41.20 \pm .07$	NGC 4073 group 136 Mpc			
NGC 388	E	10.03	<40.42	NGC 4073	E	11.49	43.11 ± 0.02
NGC 379	S0	10.63	$41.20 \pm .07$	NGC 4139	S0	10.58	<40.74
PCC S34-111:LLB96 402	E	9.56	<40.34	NGC 4063	S0	10.45	41.27 ± 0.18
PCC S34-111:LLB96 265	S0	10.29	<40.23	NGC 4077	S0	10.83	41.50 ± 0.12
NGC 524 group 50 Mpc				PGC 038154	S0	10.48	<40.77
NGC 524	S0	11.06	<40.50	NGC 4261 group 53 Mpc			
NGC 518	S	9.92	<40.08	NGC 4261	E	11.09	41.74 ± 0.04
NGC 532	S	9.99	<40.09	NGC 4264	S0	10.15	40.47 ± 0.13
NGC 533 group 107 Mpc				PGC 039655	i	9.49	<40.18
NGC 533	E	11.35	42.61 ± 0.03	NGC 4257	S	9.68	<40.17
NGC 0533:ZM98 0034	E	9.62	<40.88	PGC 039639	I	8.91	<40.17
NGC 0533:ZM98 0046	E	9.61	<40.54	PGC 039708	S0	9.64	40.22 ± 0.18
NGC 0533:ZM98 0027	E	9.55	<40.81	NGC 4269	S0	10.06	40.29 ± 0.18
NGC 0533:ZM98 0017	S	9.84	<40.50	NGC 4260	S	10.55	40.56 ± 0.13
NGC 0533:ZM98 0026	E	9.59	<40.48	VCC 0405	E	7.63	<40.16
NGC 741 group 106 Mpc				VCC 0315	S	9.64	<40.20
NGC 741	S0	11.4	41.90 ± 0.07	NGC 4266	S	9.80	<40.25
NGC 0741:ZM98 0009	E	10.19	<40.82	PGC 039532	I	9.23	<40.27
NGC 0741:ZM98 0023	E	9.43	<40.78	PGC 039711	I	8.75	<40.31
NGC 0741:ZM98 0010	E	10.07	<40.98	NGC 4287	S	9.77	<39.83
NGC 0741:ZM98 0014	S	10.03	<40.53	NGC 4325 group 163 Mpc			
NGC 0741:ZM98 0011	E	10.07	40.62 ± 0.30	NGC 4320	S	10.70	<41.33
NGC 1587 group 77 Mpc				NGC 4325:ZM98 0030	E	10.09	<41.06
NGC 1587	E	10.88	<40.79	NGC 4325	E	10.89	42.88 ± 0.06
NGC 1588	E	10.40	<40.96	NGC 4636 group 33 Mpc			
NGC 1589	S	10.84	<40.80	NGC 4636	E	11.04	42.03 ± 0.02
PGC 015369	I	8.76	<40.62	NGC 4761 group (HCG 62) 105 Mpc			
NGC 2563 group 107 Mpc				NGC 4761	S0	10.9	42.78 ± 0.02
NGC 2562	S	10.69	40.84 ± 0.17	PGC 043760	E	9.83	<40.63
NGC 2563	S0	11.04	41.7 ± 0.07	HCG 062:ZM98 0036	E	9.70	<40.58
NGC 2563:ZM98 0016	S	10.10	<40.48	HCG 062:ZM98 0022	S	9.99	41.01 ± 0.13
NGC 2563:ZM98 0033	S	9.96	<40.70	NGC 5129 group 150 Mpc			
NGC 2560	S	10.52	40.60 ± 0.27	NGC 5129:ZM98 0007	S	10.38	<41.16
PGC 023448	E	10.10	<40.47	NGC 5129	E	11.33	41.31 ± 0.25
PGC 023391	S	10.32	<40.35	NGC 5176 group 150 Mpc			
NGC 3091 group (HCG 42) 91 Mpc				NGC 5176	S0	10.38	<41.44
NGC 3091	E	11.31	42.04 ± 0.04	NGC 5177	S0	10.38	40.90 ± 0.34
NGC 3096	S0	10.36	40.48 ± 0.23	NGC 5171	S0	11.05	41.42 ± 0.30
HCG 042:ZM98 0046	S	9.27	<40.38	NGC 5179	S0	10.58	41.12 ± 0.19
NGC 3607 group 33 Mpc				NGC 5178	S0	10.63	<41.41
NGC 3608	E	10.54	<40.24	NGC 5846 group 42 Mpc			
NGC 3607	S0	10.90	40.12 ± 0.31	NGC 5845	E	10.04	<40.35
NGC 3605	E	9.97	39.71 ± 0.32	NGC 5850	S	10.82	40.57 ± 0.15
PGC 034419	S	9.42	<40.04	NGC 5839	S0	9.96	<40.35
NGC 3599	S0	10.10	<40.17	NGC 5846	E	11.07	41.51 ± 0.05
NGC 3665 group 53 Mpc				NGC 5846:ZM98 0015	S	9.20	<40.37
NGC 3665	S0	10.92	<40.61	NGC 5848	S0	9.53	<40.45
NGC 3658	S0	10.38	40.52 ± 0.31				

Table 1. The galaxy data. Names, types and B-band luminosities are derived from values given in the NED. L_X units are bolometric $\log(\text{erg s}^{-1})$, L_B units are $\log(\text{B-band Solar})$. Upper limits are 3σ above the background. Errors are 1σ and based on photon counting statistics.

Table 1 *continued*

Galaxy name	type	L_B	L_X	Galaxy name	type	L_B	L_X
NGC 6338 group 171 Mpc				HCG 48 56 Mpc			
NGC 6338	S0	11.3	43.28 ± 0.02	HCG 48a	E	10.54	40.681 ± 0.106
NGC 6345	S0	10.49	41.21 ± 0.28	HCG 48b	S	9.69	$41.459 \pm .021$
IC 1252	S	10.37	<41.19	HCG 48c	S0	9.13	<40.079
NGC 6346	E	11.16	<41.18	HCG 48d	E	8.69	<40.079
NPM1G +57.0229	S	10.29	41.02 ± 0.30	HCG 51 155 Mpc			
NGC 7619 group 65 Mpc				HCG 51a	E	10.77	$41.357 \pm .085$
NGC 7626	E	10.94	<40.68	HCG 51b	S	10.34	<40.973
NGC 7619	E	10.97	<40.91	HCG 51c	S0	10.73	41.017 ± 0.187
NGC 7617	S0	9.90	40.63 ± 0.11	HCG 51d	S	10.30	<41.033
PGC 071159	S	9.72	<40.14	HCG 51e	E	10.53	41.017 ± 0.155
NGC 7623	S0	10.26	<39.88	HCG 68 48 Mpc			
PGC 071120	S	9.65	<40.15	HCG 68a	S0	10.76	$41.017 \pm .035$
PGC 071085	E	9.96	<40.17	HCG 68b	E	10.61	<40.079
NGC 7631	S	10.24	39.75 ± 0.33	HCG 68c	S	10.69	$40.322 \pm .092$
NGC 7611	S0	10.40	40.62 ± 0.14	HCG 68d	E	9.97	<40.079
PGC 071110	S	9.61	39.93 ± 0.25	HCG 68e	S0	9.72	<40.079
NGC 7777 group 133 Mpc				HCG 90 53 Mpc			
PGC 072792	E	10.73	<41.35	HCG 90a	S	10.49	$40.518 \pm .068$
HCG 15 137 Mpc				HCG 90b	E	10.70	40.255 ± 0.119
HCG 15a	S0	10.56	40.75 ± 0.20	HCG 90c	E	10.40	40.113 ± 0.171
HCG 15b	S0	10.14	<40.81	HCG 90d	S	9.94	40.079 ± 0.156
HCG 15c	S0	10.62	<40.81	HCG 91 143 Mpc			
HCG 15d	S0	10.34	41.71 ± 0.04	HCG 91a	S	11.27	$43.164 \pm .006$
HCG 15e	S0	10.14	<40.81	HCG 91b	S	10.23	40.707 ± 0.217
HCG 15f	S	9.76	<40.81	HCG 91c	S	10.61	<40.812
HCG 16 79 Mpc				HCG 92 129 Mpc			
HCG 16a	S	10.72	40.94 ± 0.07	HCG 92c	S	10.76	41.262 ± 0.115
HCG 16b	S	10.52	40.23 ± 0.21	HCG 92e	E	10.58	40.755 ± 0.249
HCG 16c	S0	10.29	41.30 ± 0.04	HCG 97 131 Mpc			
HCG 16d	I	10.30	40.72 ± 0.10	HCG 97a	S0	10.69	41.97 ± 0.04
HCG 31 82 Mpc				HCG 97b	S	10.13	<40.812
HCG 31a	S	9.76	<40.46	HCG 97c	S	10.40	<40.875
HCG 31b	S	9.93	<40.46	HCG 97d	E	10.53	40.944 ± 0.144
HCG 31c	S	10.69	40.81 ± 0.08	HCG 97e	S0	9.72	<40.857
HCG 31d	S	8.60	<40.46				
HCG 44 28 Mpc							
HCG 44a	S	10.23	39.95 ± 0.08				
HCG 44b	E	10.35	39.65 ± 0.13				
HCG 44c	S	9.88	<39.53				
HCG 44d	S	9.51	<39.53				

4 X-RAY PROPERTIES OF LATE-TYPE GALAXIES IN GROUPS

4.1 $L_X:L_B$

Figure 1 shows the $L_X:L_B$ relation for the late-type galaxies in our sample. No significant difference in the relation is apparent between the subsamples in compact and loose groups, so we have combined the two. It is clear that two points stand out from the trend described by the rest. The upper of these is HCG 91a, a Seyfert 1 with powerful central point-like X-ray source associated with the central AGN. Since this study aims to explore the X-ray properties of *normal* galaxies, we exclude HCG 91a from fits derived below. The second high point is HCG 48b. This is not known to have an active nucleus, however it is likely that it contains some sort of active nucleus as it stands out in a similar way to HCG 91a in both Figures 1 and 2. As a result we also exclude HCG 48b from the fits derived below (although we will show its effect on the fits).

As can be seen in Figure 1 there are a large number

of upper limits, so we have used survival analysis to derive best fits to the data. Survival analysis takes into account both detections and upper limits, providing that the censoring is random – i.e. upper limits must be unrelated to the true values of the parameter being studied. (For example, this would not be the case if longer observations have been made for fainter objects). For our sample the luminosity limits are determined by both exposure time and source distance, and in almost all cases the galaxies were not the main target of the observation. Note that although galaxies in more distant groups may have been observed for longer because of lower fluxes, this does not mean that lower *luminosity* galaxies have been observed longer. Random censoring should therefore be a reasonable approximation.

Linear regression analysis was carried out using the expectation and maximisation (EM) and Buckley-James (BJ) algorithms in IRAF. The EM method requires that the residuals about the fitted line follow a Gaussian distribution, whilst the BJ algorithm calculates a regression using Kaplan-Meier residuals and only requires that the censoring

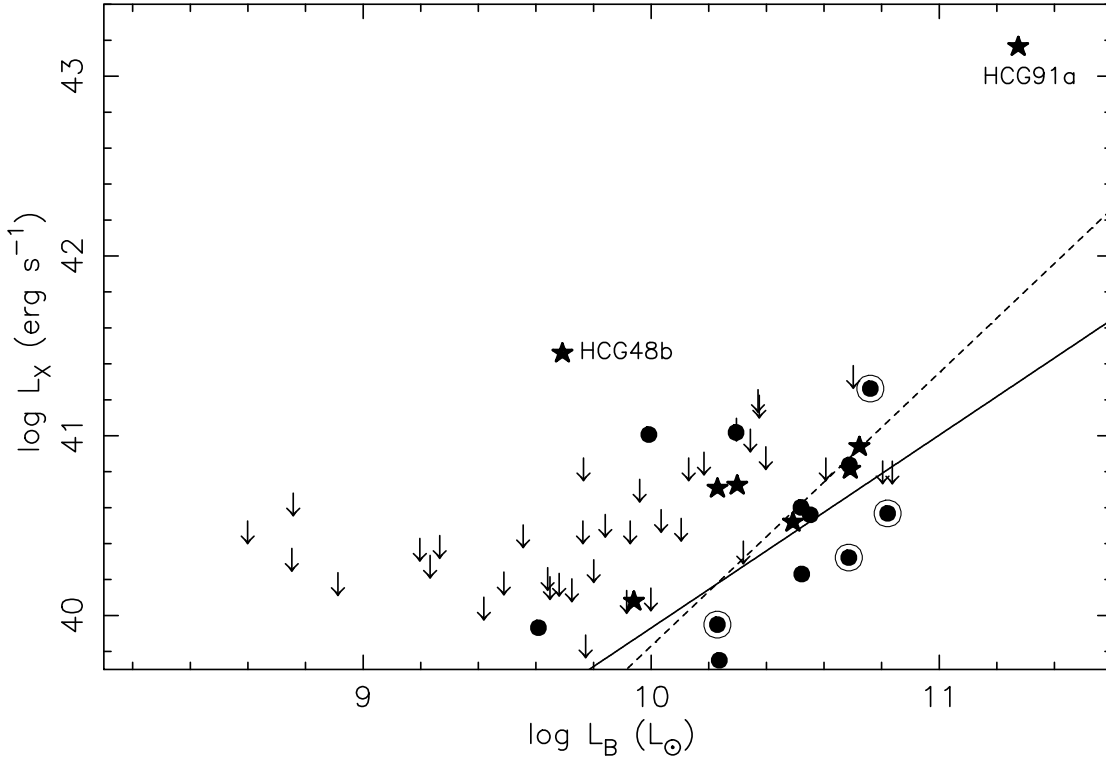


Figure 1. $L_X:L_B$ relation for the late-type group galaxies. Arrows represent upper limits, other points are detections with stars representing likely starbursts (or AGN), ringed circles non-starbursts and solid circles late-types whose activity is unknown. The solid line is the best fit to all the data, and the dashed line shows the relation as derived by Shapley et al. (2000) for a large sample of late-type galaxies observed by *Einstein*.

distribution about the fitted line is random. When fitting the lines the uncensored points were used as independent variables, and the censored points as dependent variables. In all cases in this paper the two different methods give similar results, and all quoted lines are based on the mean of these two methods. A third possible method of linear regression, Schmitt binning, was not used as the results can be unreliable in cases with heavy censoring.

The best fit line (solid) shown in Figure 1 is

$$\log L_X = (1.07 \pm 0.3) \log L_B + (29.2 \pm 2.1)$$

(the slope drops to 0.95 with HCG 48b included). For comparison we also plot the regression line of Shapley et al. (2000) who derived the $L_X:L_B$ relation for a large sample of spirals (covering a range of environments).

The Shapley et al. (2000) relationship (slope= 1.52 ± 0.1 , intercept= 24.6), whilst steeper, lies within 2σ of the slope derived here. It is therefore not clear that our results are in conflict with those of Shapley et al. (2000), especially since these authors find evidence for extra emission (possibly from a hot halo) in the largest spirals, which are mostly absent from our sample.

In galaxy groups it might be expected that galaxy interactions may result in starbursts which could increase the X-ray to optical luminosity ratio (Read & Ponman 1998). We identify starbursts on the basis of their FIR colours ($f_{60}/f_{100} > 0.4$, though note that an AGN may also have such warm FIR colours – Bothun et al. 1989). The 12 galax-

ies for which FIR colour is available show that the starbursts (or AGN) lie above the best fit line (8 galaxies including HCG 91a and HCG 48b) and the non-starbursts generally lie below the best fit line (3 out of 4 galaxies). However, this difference is not large, and the data generally suggest that some late-type galaxies in groups may have a small enhancement of their X-ray emission (relative to the optical) but overall these galaxies follow the same $L_X:L_B$ relation as galaxies in other environments.

4.2 $L_X:L_{FIR}$

In Figure 2 we plot the $L_X:L_{FIR}$ relation for the late-type galaxies in our sample. FIR luminosities are calculated from IRAS 60 and 100 μm fluxes using

$$L_{FIR} = 3.65 \times 10^5 (2.58S_{60\mu m} + S_{100\mu m})D^2 \quad (L_\odot)$$

(e.g. Devereux & Eales 1989) where D is the distance in Mpc, $S_{60\mu m}$ and $S_{100\mu m}$ are the IRAS 60 and 100 μm fluxes in Janskys. Most of the galaxies with IRAS fluxes recorded are in the Hickson Compact groups, and the flux values are taken from Hickson et al. (1989). For other galaxies, IRAS fluxes are taken from NED. Only galaxies detected in the X-ray and having a determined FIR luminosity are plotted. The dashed line in Figure 2 is from Shapley et al. (2000)

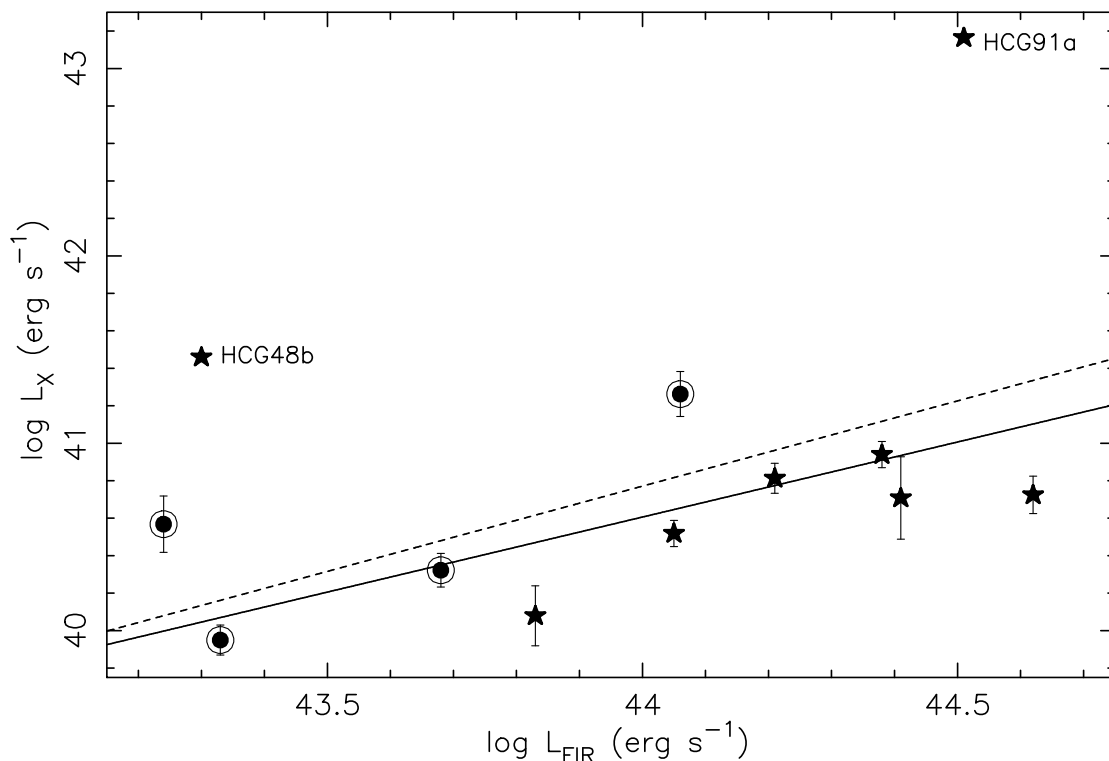


Figure 2. Late-type galaxy $L_X:L_{FIR}$ relation. Only galaxies detected in the X-ray and with determined far infrared luminosities are plotted. Stars represent starburst galaxies or AGN, and ringed circles non-starbursts. The overlaid lines are taken from fits to the spiral samples of Read & Ponman (2001) (solid line) and Shapley et al. (2000) (dashed).

and the solid line is from a smaller ROSAT PSPC survey of nearby spirals by Read & Ponman (2001).

The rather tight correlation between the two variables, which has been noted previously, is clearly apparent. The two points well away from the trend are once again HCG 91a and HCG 48b. This strongly suggests that HCG 48b, like HCG 91a, contains an AGN, since strong interaction-induced starburst activity tends to *decrease* the ratio of L_X/L_{FIR} (Read & Ponman 1998). In fact the Read & Ponman (2001) line in Figure 2 is a good fit to both normal and starburst galaxies, with starbursts occupying the high L_X (or high L_{FIR}) end of the relation. The starbursts as identified in § 4.1 above do indeed tend to lie in this region of the relation. Despite the limited number of data points it can be seen that most late-type galaxies in groups again follow the same relation as spirals in other environments.

5 X-RAY PROPERTIES OF EARLY-TYPE GALAXIES IN GROUPS

Figure 3 shows the $L_X:L_B$ relation for the early-type galaxies in our sample. No significant difference is apparent between the compact and loose group samples. The crossed circles represent the non-central group galaxy detections and the arrows upper limits. Shaded squares are central-dominant group galaxies, as defined in § 3.2.1 and include HCG 97a, which is a central-dominant galaxy from the HRI sample. Also plotted for comparison are the best fit to the

early-type galaxy $L_X:L_B$ relation as determined by Beuing et al. (1999), on the basis of their study of a large sample of early-type galaxies derived from the ROSAT All Sky Survey (RASS), and an estimate of the discrete source contribution. This latter estimate was derived using the mean hard component L_X/L_B derived by Matsushita et al. (2000). These authors used spectral fits to ASCA data to calculate the contribution of the hard spectral component, identified with discrete galactic sources, in the 0.5-10 keV band, assuming a 10 keV thermal bremsstrahlung model for its spectrum. As we use a 1 keV Raymond & Smith (1977) model for all our galaxies we have converted the Matsushita et al. (2000) L_X/L_B ratio to our assumed model and bandpass to give a discrete source estimate of $L_X/L_B=29.56$. This value is in reasonable agreement with a number of other estimates of this hard discrete source contribution, once the effects of differing bandpasses and models are taken into account (Canizares et al. 1987; Ciotti et al. 1991; Matsumoto et al. 1997; Irwin & Sarazin 1998). It can also be seen to constitute a reasonable lower envelope for the X-ray luminosity of the galaxies in our sample. It has been suggested that there is also a very soft component associated with discrete sources (e.g. Irwin & Sarazin 1998). If this component is present in all galaxies its effect on our estimated discrete source contribution would be somewhat dependent on the absorbing column, but could typically increase it by a factor of ~ 2 . However, recent Chandra observations have resolved much of the discrete source contribution in early-types (Sarazin

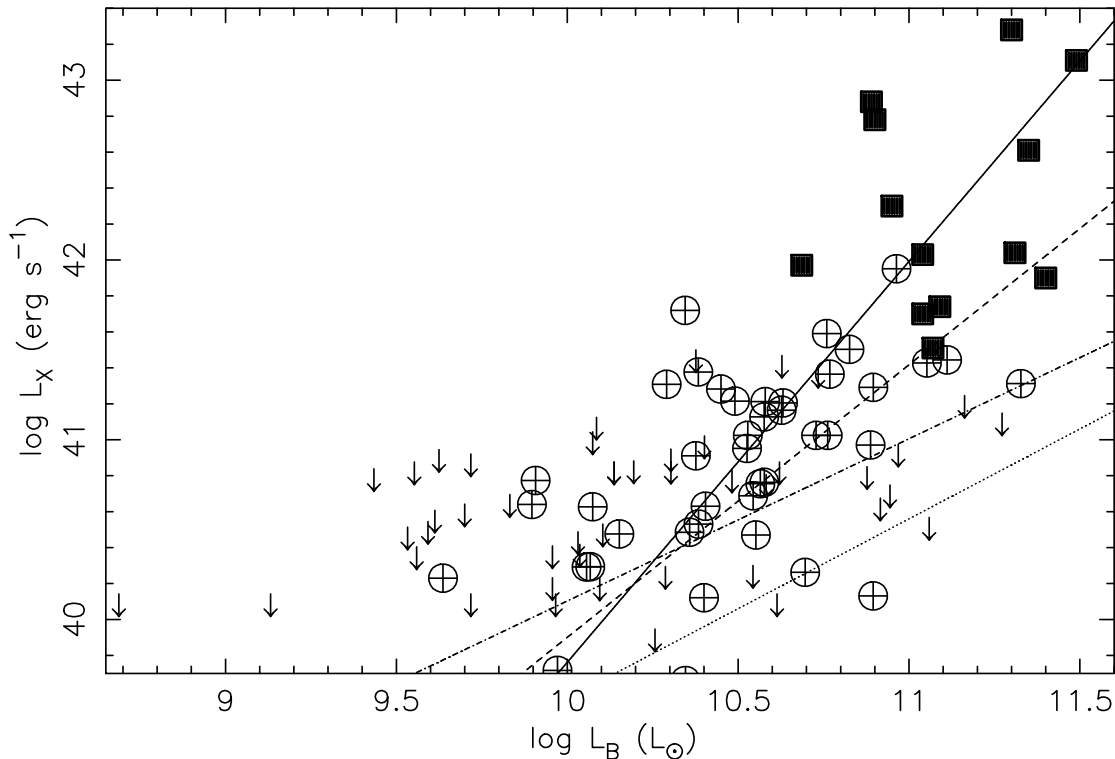


Figure 3. $L_X:L_B$ relation for the early-type group galaxies. The filled squares represent the central-dominant group ellipticals, the circles with crosses represent other detected early-type galaxies in groups, and the arrows are upper limits. Also plotted on the graph are the following lines, the $L_X:L_B$ relation as derived by Beuing et al. (1999 - solid line), an estimate of the discrete source contribution (dotted line), the best fit to the full group galaxy sample (dashed line) and the best fit to the group sample excluding central dominant galaxies (dot-dash line).

et al. 2000; Blanton et al. 2000), and Chandra spectral analysis of this discrete component show that any soft component is very weak relative to the hard component (Blanton et al. 2000).

As described in § 4.1, we again use survival analysis to derive fits to the data, including the upper limits available. Fitting to the whole dataset gives

$$\log L_X = (1.5 \pm 0.2) \log L_B + (24.7 \pm 2.0)$$

which is plotted as the dashed line in Figure 3. Although this fit is flatter than the Beuing et al. (1999) line (slope = 2.23 ± 0.12), a large fraction of our data lie in the region $\log L_X \leq 40.5$. Below this luminosity previous work indicates that the slope of the relation is approximately unity (Eskridge et al. 1995), we therefore expect a somewhat flatter slope than derived by Beuing et al. (1999), who had many more luminous galaxies in their sample. In fact if we restrict the fit to the more optically luminous galaxies the slope does indeed steepen to ~ 2.2 (and if we restrict the Beuing et al. (1999) data to the less optically luminous galaxies their slope flattens).

However it is clear that the central-dominant group galaxies all lie in the upper right region of the graph. This along with their central position in the group suggests that they may not be typical of other early-type group galaxies.

Thus we also fit a regression line to the data after excluding all central-dominant galaxies, obtaining a best fit of,

$$\log L_X = (0.90 \pm 0.18) \log L_B + (31.1 \pm 1.8)$$

which is significantly flatter than the previous fit and is plotted as the dot-dash line in Figure 3.

While the fit to the full dataset does appear to be consistent with previous work, of more interest is the very flat slope obtained if the central-dominant group galaxies are excluded. Since this line has a slope consistent with unity, one interpretation might be that the X-ray emission is primarily from stellar sources, and that these non-central group galaxies do not contain a significant hot halo. However the level of this line is a factor ~ 2.5 above the expected hard discrete source contribution, and even if a soft component is included in the discrete source contribution, many of these galaxies will still lie above the line, suggesting that a hot halo still remains. We will return to this issue below.

A further factor which might be influencing our result, which is significantly flatter than that derived in previous studies (e.g. Beuing et al. 1999; Eskridge et al. 1995), is that these other studies included galaxies from a range of environments, whilst we have specifically targeted galaxies in X-ray bright groups. To explore this, we now compare group galaxies to those in low density environments.

6 COMPARISON WITH NON-GROUP EARLY-TYPE GALAXIES

To investigate the effects of environment on the properties of early-type galaxies we adopt two approaches. Firstly we use a previous large study of the X-ray properties of early-type galaxies. This large sample will be used to derive group and field subsamples, and the properties of each subsample examined. The second approach involves defining a sample of very isolated early-type galaxies whose properties we can compare with our group galaxies. This latter approach results in a smaller sample, but with much more reliable X-ray parameters. Both approaches are described in detail below.

6.1 Environmental effects in the RASS sample

The largest ROSAT study to date of early-type galaxies is that of Beuing et al. (1999), with nearly 300 galaxies examined using X-ray data from the RASS. However one complication in the Beuing et al. L_X values is the presence of intragroup or intracluster X-ray emission which Beuing et al. associate with the galaxy if it lies at the centre of the extended X-ray emission. This will tend to increase the quoted L_X for high luminosity galaxies (which are especially likely to lie in clusters, or in the cores of galaxy groups), increasing the slope of the L_X/L_B relation at high L_B values.

In order to investigate any possible environmental dependence in the Beuing *et al.* sample we divided the sample into a number of group and field subsamples. Cluster galaxies were identified and removed based on membership in the Abell et al. (1989) and Faber et al. (1989) catalogues. The X-ray properties of cluster galaxies determined by Beuing et al. may be severely contaminated by cluster emission, and will be best addressed by future observations with the high spatial resolution of Chandra. These are not the object of the present study. Group membership is taken from the all sky group catalogue of Garcia (1993), which has a velocity limit of $5,500 \text{ km s}^{-1}$. Any galaxy not classified as a member of a cluster or group from these catalogues is considered to be in the field. Galaxies more distant than $5,500 \text{ km s}^{-1}$ are removed to avoid possible misclassification. This process produces 127 group galaxies and 81 in the field. To explore any possible difference between central-dominant group galaxies and other galaxies in groups, we further split the Beuing et al. group sample into a sample of BGGs and one with all BGGs removed.

Beuing et al. (1999) record the radii to which they detect emission around each galaxy. In an attempt to explore the effects of contamination of their galaxy fluxes by surrounding group emission, we also split the group sample into subsamples with extents greater than and less than 200 kpc. Galaxies with extents $> 200 \text{ kpc}$ are very likely to include a significant amount of group emission.

We fitted the $L_X:L_B$ relation for each subsample separately using survival analysis techniques as described earlier. The results for the slopes of these fits for non-cluster galaxies are shown in Table 2. These results do appear to indicate the presence of significant environmental effects, with the BGG galaxies having a very steep slope, the field sample a flatter relation, and group galaxies with emission confined within 200 kpc a flatter slope still. However some of these

fits may be biased, since some of the subsets have very few detections and many upper limits.

In order to reduce any bias in our comparisons we binned our data into optical luminosity bins and used the Kaplan-Meier estimator (which includes upper limits) within IRAF to derive the mean value of L_X/L_B for each bin. This technique works by redistributing the contribution from each upper limit over all the lower points within a bin. One effect of this, is that estimates may be seriously biased where all the lowest values within a bin consist of upper limits. To avoid this problem, we discard bins which have many more upper limits than detections. In Figure 4 we plot $\log(L_X/L_B)$ versus $\log L_B$ for the subsets of the Beuing et al. (1999) data. There is some evidence from this plot that the BGGs (which often have $r_{ext} > 200 \text{ kpc}$ in Beuing et al. 1999) are more X-ray luminous in general than the other early-type galaxies in groups, or the field galaxies, though the comparison is hampered by a lack of detections for non-BGG group galaxies. The rather high non-BGG point at $\log(L_B) = 11.05$ includes only 4 detections all of which show emission extending to a radius well over 200 kpc. This suggests that the fluxes for these galaxies may include a significant amount of group emission.

The field galaxy sample shown in Figure 4 could also be contaminated. The ‘field’ designation here relies on galaxies not appearing in the group catalogue of Garcia (1993). It could therefore include galaxies which are not all that isolated. In addition, the field sample could be contaminated with ‘fossil groups’ (Ponman et al. 1994; Mulchaey & Zabludoff 1999; Vikhlinin et al. 1999). These would tend to lie in the high L_B region of the plot, as they are thought to be the result of a number of galaxy mergers within a compact group, thus leaving a single bright early-type in the centre of the group potential, with no other bright galaxies nearby. Such systems can have very high X-ray luminosities, arising from the hot intergalactic medium of the erstwhile group.

The conclusion from this section is that there does appear to be some evidence for environmental effects within the Beuing et al. (1999) sample, but that the statistics are limited, the quality of the L_X values questionable, and there is some doubt about some of the environmental classification of some galaxies. To address these concerns, we now attempt to identify a sample of genuinely isolated galaxies with available X-ray data, which can be compared with our group sample.

6.2 Isolated galaxies compared with group galaxies

First we need to define a sample of isolated early-type galaxies. This was done using the Lyon-Meudon Extragalactic Data Archive (LEDA). This catalogue contains information for about 100,000 galaxies, of which $\sim 40,000$ have enough information recorded to be of use to us. From this sample we select galaxies which fit the following criteria:

- Morphological type $T \leq -3$.
- Virgo corrected recession velocity $V \leq 9000 \text{ km s}^{-1}$.
- Apparent magnitude $B_T \leq 14.0$.
- Not listed as a member of a Lyon Galaxy Group (Garcia 1993).

Dataset	Slope	Intercept	no. galaxies
Field galaxies	2.1 ± 0.4	17.8 ± 4	64(11)
Group galaxies (only BGGs)	3.5 ± 0.6	2.6 ± 7	50(24)
Group galaxies (no BGGs)	2.1 ± 0.2	18.2 ± 4	84(17)
Group galaxies with emission ≥ 200 kpc	2.7 ± 0.3	11.4 ± 4	25(25)
Group galaxies with emission < 200 kpc	1.4 ± 0.4	25.0 ± 4	109(16)

Table 2. Results of survival analysis fitting on each of the environmental subsets of the Beuing et al. (1999) sample. The first number in the 4th column is the total number of galaxies, the number in the brackets is the number of detections.

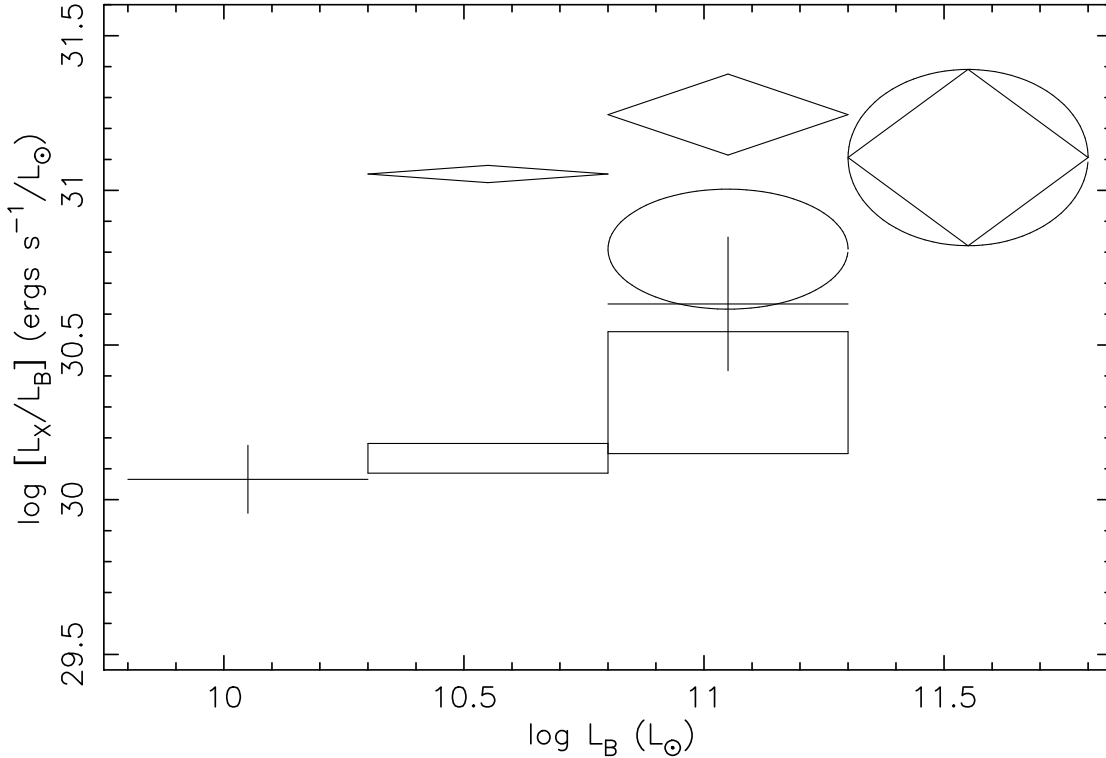


Figure 4. L_X/L_B versus L_B for the binned data from the Beuing et al. (1999) subsets. Ellipses represent BGGs, crosses non-BGG group galaxies, and light boxes field galaxies. Diamonds are group galaxies with emission recorded as being >200 kpc in extent.

The restrictions on apparent magnitude and recession velocity are imposed to minimize the effect of incompleteness in the catalogue. The LEDA catalogue is known to be 90% complete to $B_T = 14.5$ (Amendola et al. 1997), so our sample should be close to being statistically complete.

This selection gives 330 galaxies which can be considered as potential candidates. These are compared to the rest of the catalogue and accepted as being isolated if they have no neighbours which are:

- within 700 km s^{-1} in recession velocity.
- within 1 Mpc in the plane of the sky.
- less than 2 magnitudes fainter in B_T .

These criteria are imposed to ensure that galaxies do not lie in groups or clusters and that any neighbours they do have are too small to have had any significant effect on their evolution and X-ray properties.

To check the results of this process, all galaxies are compared against NED and the Digitized Sky Survey (DSS). A NED search in the area within 1 Mpc of the galaxy picks out galaxies which are not listed in LEDA, and examination of the DSS reveals any galaxies of similar brightness to the candidate which are not listed in either catalogue. We believe that these measures ensure that the isolation of the galaxy is real, and not produced by errors or omissions in the catalogue. Our final sample consists of 36 isolated early-type galaxies.

Comparison of these 36 galaxies with previously published work, and with pointed X-ray observations (*ROSAT*, *ASCA* & *Einstein*) reveals that only 8 have X-ray data available. Of these, two (NGC 821 and NGC 2271) have been observed in the ROSAT All-Sky Survey (RASS), but were not detected at 3σ confidence, and have no pointed observations available. NGC 6776 is a fairly recent post-merger (Sansom

Name	Distance (km s ⁻¹)	Hubble Type	B_T (mag)	D_{nn} (Mpc)	X-ray Data	log L_X (erg s ⁻¹)	L_X/L_B	notes
NGC 821	1747	-4.8	11.74	>1	RP	<40.94	<30.25	RASS
NGC 1132	6904	-4.9	13.26	>1	A	~43.0	~31.84	MZ99
NGC 2110	2091	-3.0	13.40	>1	A	42.1	32.04	Seyfert 2
NGC 2271	2412	-3.2	13.24	>1	RP	<41.12	<30.43	RASS
NGC 2865	2451	-4.1	12.41	>1	RP	<40.76	<30.22	RASS
NGC 4555	6775	-4.8	13.31	>1	RP	41.15	30.03	Satellites
NGC 6776	5281	-4.1	13.01	>1	RP	41.18	30.15	post-merger
NGC 7796	3145	-3.9	12.42	>1	RP	41.58	30.76	
NGC 993	6967	-3.4	14.64	0.67	RP	<41.77	<30.14	
NGC 2418	5066	-4.9	13.34	0.4	RP	41.36	30.49	
IC 3171	7096	-3.3	14.60	0.4	RP	<41.40	<30.75	
CGCG 196-012	8897	-3.0	15.52	0.53	RP	<41.92	<31.34	
MCG +3-47-10	5249	-3.0	14.78	>1	E	<41.97	<31.65	
MCG +5-31-79	7522	-3.7	15.31	0.55	A	<42.73	<32.31	
MCG +5-31-151	7153	-3.8	14.42	>1	A	<41.95	<31.21	

Table 3. Isolated Early-type Galaxies with X-ray data. E is *Einstein*, A is *ASCA*, RP is *ROSAT* PSPC. D_{nn} is the distance in the plane of the sky to the nearest neighbour of similar magnitude and recession velocity. The L_X value for NGC 1132 is from Mulchaey & Zabludoff (1999) and values for NGC 821, NGC 2271 and NGC 2865 are taken from the *ROSAT All-Sky Survey* sample of Beuing et al. (1999). L_X for NGC 2110 is taken from Boller et al. (1992). All L_X values apart from those of NGC 6776, NGC 1132 and NGC 2110 are based on fits with fixed 0.25 solar abundance and 1keV temperature.

et al. 1988) as is NGC 2865 (Hau et al. 1999), NGC 2110 is a Seyfert galaxy, and NGC 1132 is a possible “fossil” group elliptical (Mulchaey & Zabludoff 1999). There is also a possible problem with NGC 4555, in that the DSS shows several small galaxies projected near it. Although they are probably not large enough to exclude NGC 4555 from consideration, their possible effect on the galaxy should not be ignored.

To expand and improve this subset, we chose to relax the isolation conditions and the apparent magnitude cut. We thus include galaxies that are either less isolated (no neighbours within 0.4 Mpc in plane of sky) or which are faint enough for their isolation to be uncertain ($B_T > 14$). Although these do not fit our rigorous criteria, we believe that they are isolated enough to provide useful extra information. The relaxed criteria should still exclude galaxies in truly dense environments, but might include galaxies in loose associations or in the outer fringes of large clusters. Once again we searched for X-ray data from either *ROSAT*, *ASCA* or *Einstein*.

Galaxies defined as isolated by the rigorous definition are listed in the top half of Table 3, and additional galaxies are given in the lower half. X-ray luminosities for these galaxies were derived using a simple standard reduction. The instrument from which the data were obtained for each galaxy is listed in Table 3. Luminosities from *ROSAT* were background subtracted and corrected. Spectra were extracted from an aperture of radius ~ 6 effective radii. Detections and upper limits were derived using a Raymond-Smith plasma (Raymond & Smith 1977) model with hydrogen column fixed at Galactic values (Stark et al. 1992), temperature fixed at 1 keV and 0.25 solar metallicity.

Analysis of *ASCA* data was carried out using the screened data sets available from LEDAS (Leicester Database and Archive Service). Spectra were extracted us-

ing the XSELECT package in FTOOLS and fitted using XSPEC. In cases where no reasonable fit could be obtained and no source was obvious, we used the count rate within the circular aperture to estimate a $3\sigma_b$ upper limit on the galaxy luminosity. Conversion of count rate into flux was performed using W3PIMMS. Analysis of the *Einstein* data was performed using a reduced dataset available on CDROM from the Smithsonian Astrophysical Observatory. This did not give a detection, and a $3\sigma_b$ upper limit was derived based on the number of counts found in a $6 r_e$ radius around the galaxy position.

The $L_X:L_B$ values for the isolated galaxies are plotted in Figure 5. Also plotted for comparison are the lines shown in Figure 3. The crosses mark detections, and the corresponding galaxy names are given on the plot. Upper limits are denoted by arrows. One point of interest is that the “fossil” group elliptical (NGC 1132) lies in the same region of the plot as the central-dominant group galaxies. Note that NGC 2110 is a Seyfert galaxy.

As can be seen, the small numbers of isolated galaxies do not provide strong constraints on the $L_X:L_B$ relation. As a result we now bin up the data for the isolated galaxies, and for the group galaxy data derived in this paper. We have binned these in the same way as for the Beuing subsets in § 6.1. Figure 6 shows $\log(L_X/L_B)$ versus $\log L_B$ for the group dominant galaxies, non-central galaxies and isolated galaxies. Due to their special nature, we have excluded the fossil group and the Seyfert from the isolated galaxy sample. No bins in the group samples are omitted due to poor statistics this time. This Figure shows a much clearer picture than the results derived above from the Beuing sample. The L_X/L_B ratio for non-central group galaxies and isolated galaxies is consistent with a constant $\log L_X/L_B$ value of ≈ 30 (erg s⁻¹ L_\odot^{-1}), whilst the central dominant group galax-

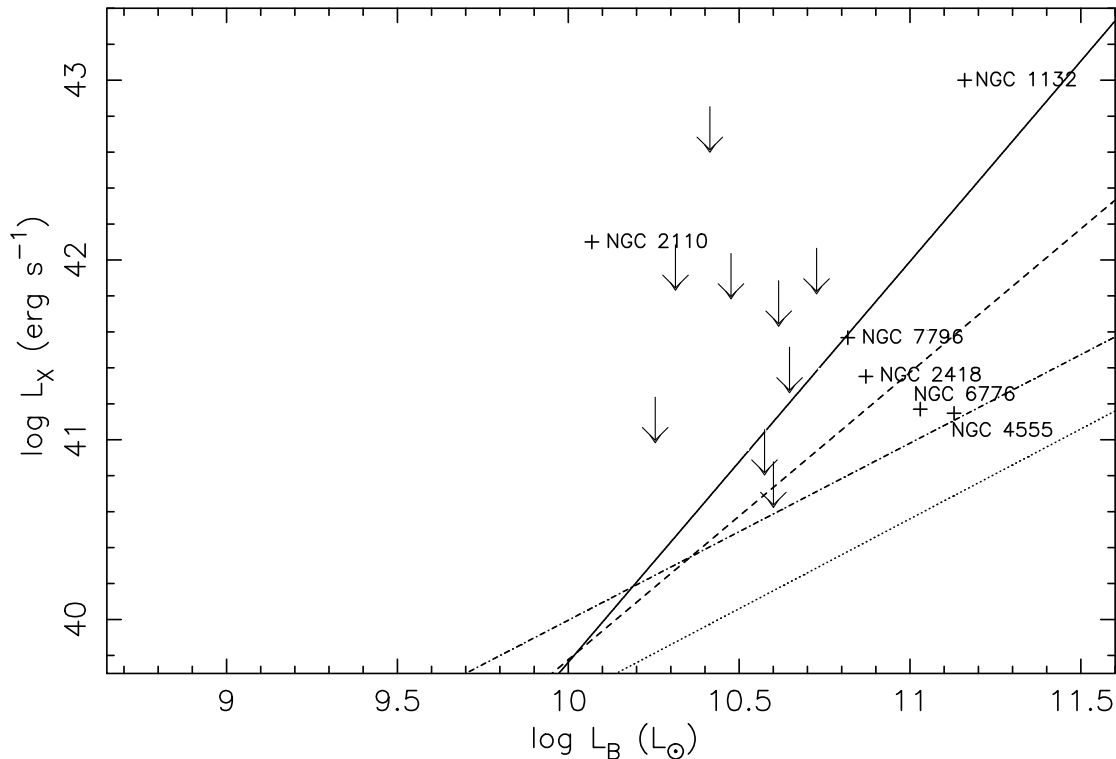


Figure 5. $L_X:L_B$ relation for our sample of isolated early-type galaxies. The labeled crosses mark the detections and the arrows the upper limits. The lines plotted are the same as those in Figure 3.

ies are clearly far more X-ray luminous than other galaxies of similar optical luminosity.

The significant X-ray over-luminosity of the central group galaxies relative to the others, suggests that some process is enhancing the X-ray emission from these central galaxies, whilst other early-type galaxies in groups are similar in their X-ray properties to isolated galaxies.

7 DISCUSSION

There are two main results from the data presented above. Firstly, the X-ray properties of spirals in galaxy groups appear to be indistinguishable from spirals in other environments. Secondly, the X-ray properties of early-type galaxies in groups appear to depend on whether the galaxy is centrally located or not.

The properties of the late-type galaxies in groups are perhaps unsurprising, given that in late-type galaxies much of the X-ray emission is believed to come from stellar sources. Spirals which lie significantly above the $L_X:L_B$ relation most likely contain active nuclei, and also show excess X-ray emission relative to the $L_X:L_{FIR}$ relation. The solid line plotted in Figure 2 is a good fit to both normal and starbursting galaxies (Read & Ponman 2001) suggesting that the excess X-ray emission seen in HCG 91a and HCG 48b is not due to starbursts.

In the case of compact groups, there is strong evidence that the group environment leads to galaxy interactions

(Mendes de Oliveira & Hickson 1994), but the statistical evidence that this leads to increased starburst activity is controversial (see e.g. Hickson 1997; Shimada et al. 2000). Our results do not throw any additional light on this debate, since we do not have a well-controlled statistical sample. Rather, the implication of our results is that the X-ray luminosity of group galaxies, arising from a combination of discrete sources and starburst-related hot gas (see Read & Ponman 1998), scales with galaxy size and starburst activity, in a way which appears indistinguishable from field spirals.

In the case of early-type galaxies, our results imply that these need to be separated into two classes – central-dominant galaxies, and others – and that the failure to recognise this distinction has compromised much previous work on the X-ray properties of early-type galaxies.

What is the origin of this distinction in properties? Central-dominant group galaxies appear to be located at the centre of the group potential both in radial velocity and on the sky (Zabludoff & Mulchaey 1998). This suggests that these galaxies are not moving significantly with respect to the group potential, in contrast to other group galaxies. A galaxy moving through the intragroup medium may undergo ram pressure stripping (Gunn & Gott 1972) or viscous stripping (Nulsen 1982). Simulations of galactic halos in clusters also suggest that tidal stripping by the cluster potential can remove a significant amount of a galaxy halo (Okamoto & Habe 1999). All these processes could reduce the amount of hot gas that the galaxy could retain, thus reducing the X-ray luminosity towards the value expected from stellar sources

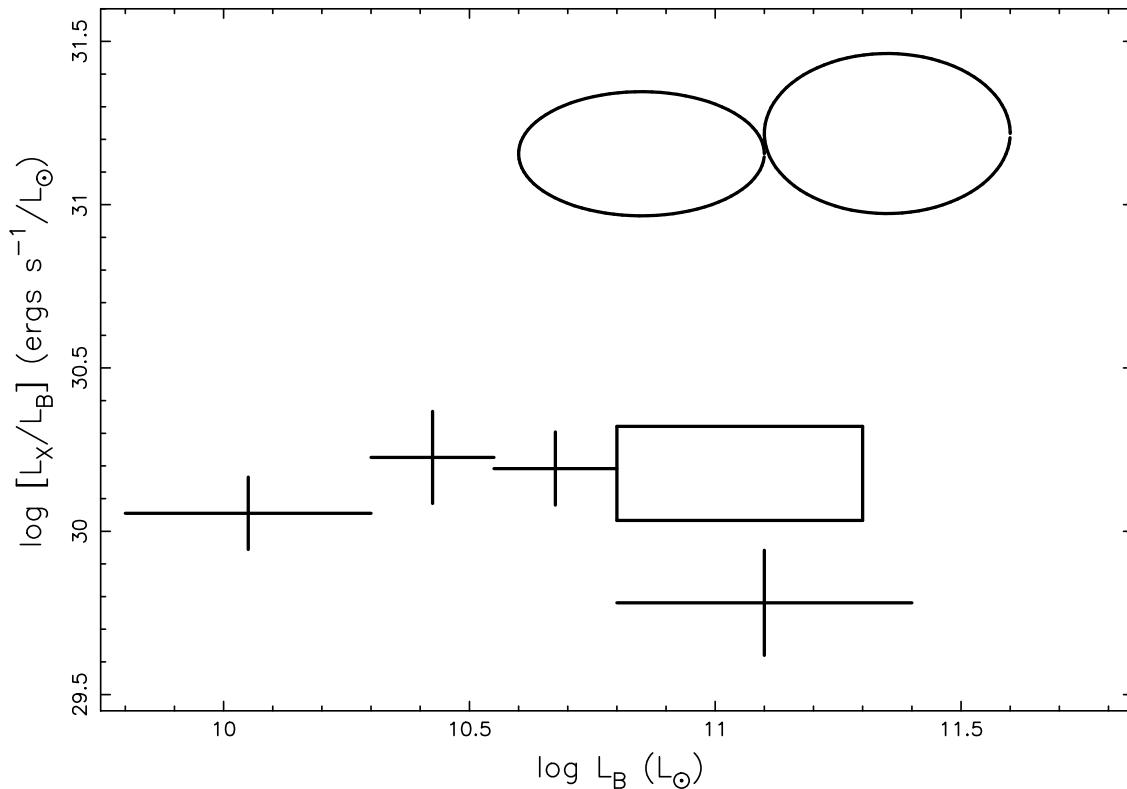


Figure 6. L_X/L_B versus L_B for the binned data for group and isolated early-type galaxies derived in this paper. Ellipses represent central-dominant group galaxies, crosses non-central group galaxies and the box isolated galaxies.

alone. In contrast, a centrally located, stationary galaxy may be able to accrete additional gas from the surrounding group potential, enhancing its X-ray luminosity.

In the absence of active stripping, the hot gas content of an early-type galaxy is determined by the balance between gas loss from stars, gas infall from the surroundings, and energy sources (notably type Ia supernovae) within the galaxy which control the energetics of the gas. The result can be a hydrostatic halo with a cooling flow, a global outflow, or a ‘partial wind’ in which an outer wind region surrounds a central inflow (Ciotti et al. 1991; Pellegrini & Ciotti 1998; Brighenti & Mathews 1999). In the case of global inflows, the X-ray luminosity is essentially equal to the whole of the injected supernova luminosity (and even higher if gas flows in from outside the galaxy), whilst in the case of winds, much of this energy may be lost in kinetic energy, and L_X is typically much lower.

Previous discussion of the observed $L_X:L_B$ relation in terms of such models, has started from the basis that this relation is steep (approximately $L_X \propto L_B^2$) for optically bright early-type galaxies. Brown & Bregman (2000), for example, suggest that the observed $L_X:L_B$ relation may be explained by a model based on the transition between galaxies with total winds, partial winds and those in which the gas is retained. They calculate that this transition should occur over the range $10.7 < \log L_B < 11.2$, leading to a rise in L_X/L_B across this range. In a galaxy group the surrounding intra-group medium might be expected to help suppress galaxy winds, pushing the region of steep L_X/L_B to lower luminosities.

However for our sample of non-central-dominant group galaxies, the average ratio of L_X/L_B is approximately constant over the range $9.8 < \log L_B < 11.3$.

What of the effects of environment on early-type galaxies? Our results (Figure 6) show no significant difference between isolated galaxies, and non-central group galaxies. In contrast, the studies of White & Sarazin (1991) and Brown & Bregman (2000) both found that the X-ray properties of early-type galaxies have some dependence on environment, but in opposite senses. Brown & Bregman (2000) find that on average, galaxies in denser environments (as defined by the Tully volume density parameter ρ) are more X-ray luminous. In fact they see that galaxies in low density environments have low L_X/L_B , whilst those in denser environments show a larger scatter in L_X/L_B . In the light of our results, it is natural to ask whether this result might be entirely due to the inclusion of central-dominant group galaxies in the Brown & Bregman (2000) sample. In the Beuing et al. (1999) sample, only 3 out of 58 galaxies with $\log L_B > 11.0$ are found in the field. This suggests that almost all optically bright early-type galaxies are located in groups and clusters. Many of these brightest galaxies will be central-dominant group galaxies, which will naturally lie in rather dense environments, and have a high value of L_X/L_B .

If we remove all the brightest group galaxies from the Brown & Bregman (2000) sample (optically brightest as defined by Garcia 1993 plus two from Helsdon & Ponman 2000) the trend in L_X/L_B is considerably reduced. If galaxies identified as being at the centre of sub-clumps within Virgo

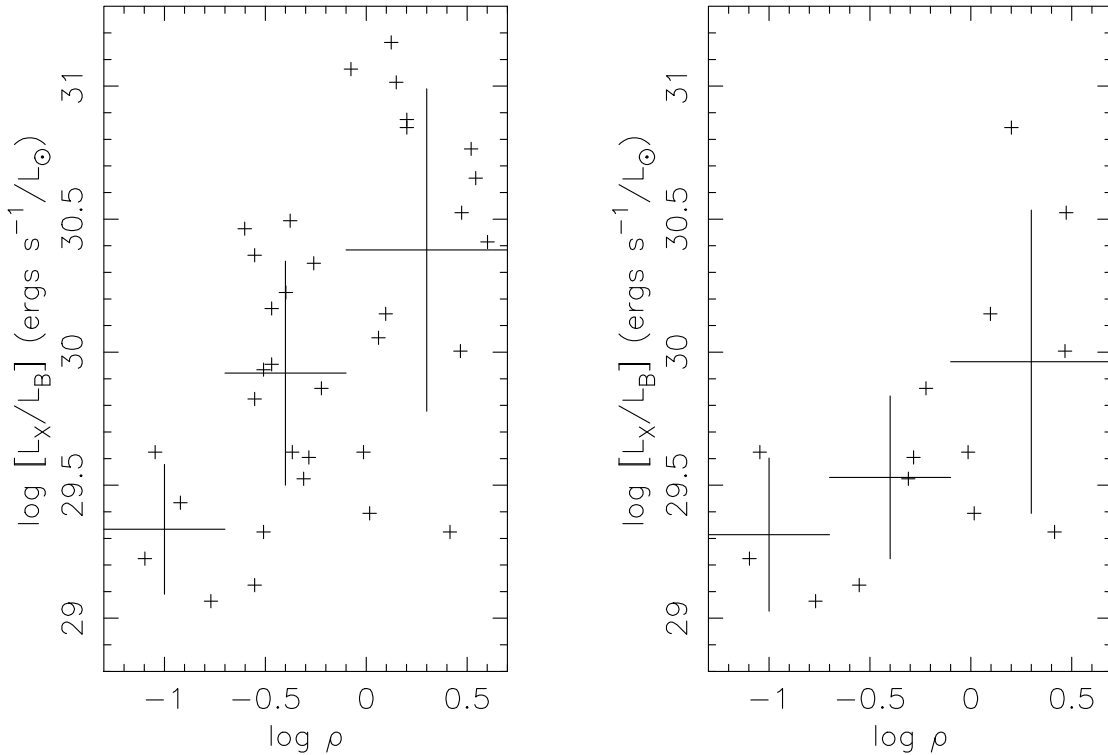


Figure 7. On the left is the original data from Brown & Bregman (2000) showing a trend of increasing L_X/L_B with galaxy volume density, ρ . On the right is the same relation but with all brightest group galaxies removed. On both plots the small crosses are galaxy data points and large crosses are binned up data.

(Schindler et al. 1999) are also removed (they may represent the cores of groups which have fallen in) the remaining data show only a weak trend ($\sim 1.5\sigma$) with galaxies in the densest environments showing a lot of scatter, while galaxies in other environments show an almost constant L_X/L_B . This is shown in Figure 7, which contrasts the original Brown & Bregman (2000) dataset with the same data with central group galaxies removed (note that an approximate conversion to our bolometric X-ray bandpass have been carried out on the data). The two highest points remaining within the high density bin are in clusters (Virgo and Fornax), and with the exception of these, the data show that non-central-dominant group galaxies across a range of environments have L_X/L_B ratios with rather little variation (scatter is factor of ~ 3 about a mean value of $\log L_X/L_B \approx 29.5 \text{ ergs s}^{-1} L_\odot^{-1}$ - we believe this value is lower than our value of $\log L_X/L_B \approx 30 \text{ (erg s}^{-1} L_\odot^{-1})$ because Brown & Bregman (2000) use 4 times the optical effective radii to extract the X-ray flux, which may actually be more extended than this). Thus much of the trend seen by Brown & Bregman (2000) is actually due to the central-dominant group galaxies. In a new study of a larger sample, O’Sullivan et al. (2000) find no trend in L_X/L_B with ρ for a sample of 196 early-type galaxies which includes almost all the Brown & Bregman (2000) galaxies.

Our result, then, is that early-type galaxies outside clusters, apart from central-dominant galaxies in groups, have an apparently universal mean value of L_X/L_B , which shows

little sign of variation with either optical luminosity or density of environment. Earlier results to the contrary appear to be due to the effects of including high luminosity central-dominant galaxies, or from contamination of L_X values by intragroup emission. Once central-dominant galaxies are excluded, the scatter in L_X/L_B is reduced, but as can be seen in Figure 8, it is still substantial, varying over a factor of 20-30 for galaxies of a given optical luminosity.

It is interesting to compare the observed L_X/L_B values with the three lines marked on Figure 8. The horizontal dotted line marks the expected discrete source contribution, discussed in section 5. Whilst this line lies close to the lower bound of the data, we note that a number of galaxies do fall somewhat below it. Irwin & Sarazin (1998) also point out that their derived discrete source contribution shows apparently real variations, by a factor of at least three, from one galaxy to another. Attributing this component primarily to low mass X-ray binaries, they argue that such variations may reflect the abundance of neutron star remnants in a galaxy, which in turn is sensitive to the initial mass function of its stars.

The upper horizontal line in Figure 8 corresponds to the energy available from type Ia supernovae. This line is derived using the Cappellaro et al. (1999) rate of $(0.18 \pm 0.06) h_{75}^2$ supernovae per century per $10^{10} L_{B\odot}$, where $h_{75} = H_0/75 \text{ km s}^{-1} \text{ Mpc}^{-1}$. Assuming that each supernova releases 10^{51} ergs of energy, this corresponds to $L_{SN}/L_B = 2.5 \times 10^{30} \text{ erg s}^{-1} L_\odot^{-1}$. This line lies within the distribution of

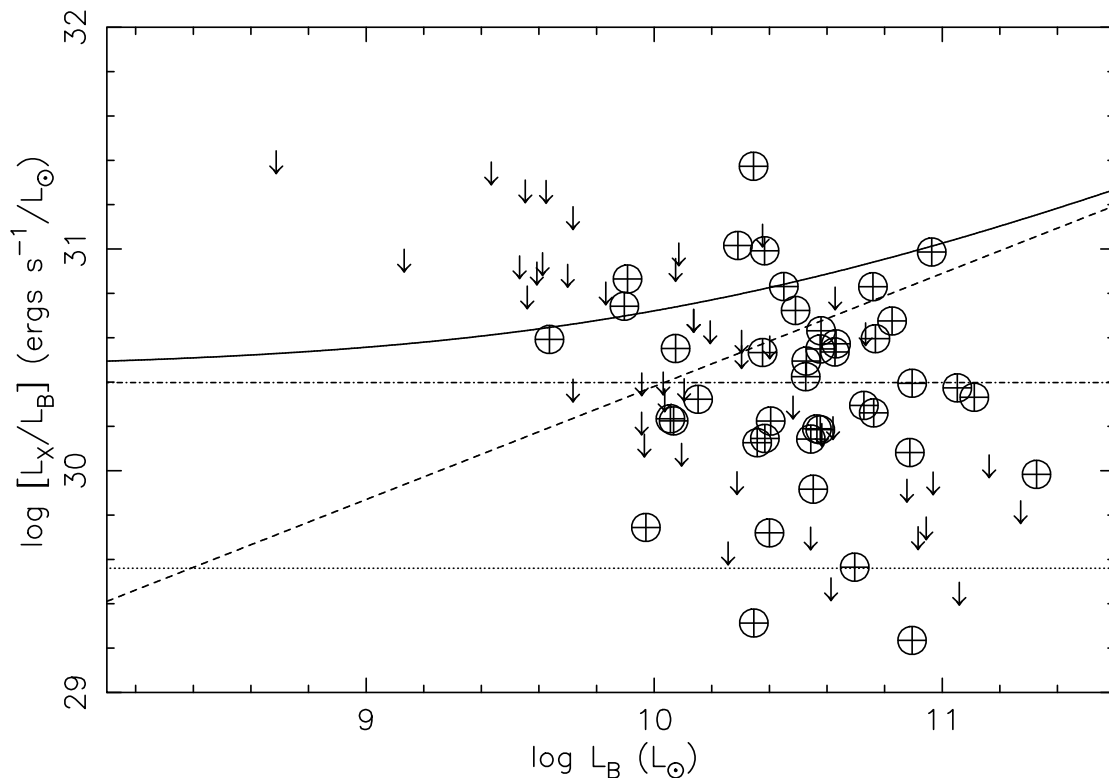


Figure 8. $\log L_X/L_B$ vs $\log L_B$ for the non central galaxies. Dotted line is estimate of discrete source contribution, dot-dash line is estimate of energy available from SNIa, dashed line is estimate of available energy due to gravitation, and the solid line is the sum of the previous three lines.

points, a factor ~ 2.5 above the characteristic mean value of $10^{30} \text{ erg s}^{-1} L_{\odot}^{-1}$ (Figure 6). What is the source of the additional luminosity in those galaxies which lie above the SNIa line? There should be a contribution from the velocity dispersion of mass-losing stars (the stellar ejecta have an initial bulk kinetic energy which will be thermalised in the surrounding interstellar medium) and another from the gravitational work done as the gas cools and flows towards the centre of the galaxy (Canizares et al. 1987; Brown & Bregman 1998). Both these contributions scale as the square of the velocity dispersion. Using the Faber-Jackson relation from Prugniel & Simien (1996), and following the analysis of Canizares et al. (1987), adopting a King profile galaxy and assuming that the gas flows into the centre before cooling out ($f = A = 1$ in their terminology), we obtain the ‘gravitational’ line, $\log L_{grav} = 25.28 + 1.51 \log L_B$, marked in Figure 8, which is uncertain by a factor of a few, depending on the radius at which gas drops out of the cooling flow, and the mass of the dark galaxy halo.

Adding the discrete source, SNIa and gravitational terms gives an upper envelope for L_X/L_B , which is shown in Figure 8. Three of the four galaxies which lie significantly above this line in the plot are all peculiar. The highest, HCG 15d, is an interacting galaxy which also a radio source. The HRI emission from this galaxy is dominated by a central point-like source which is most likely an AGN. The two galaxies above the line with $\log(L_X/L_B) \approx 31$ and $\log L_B \approx 10.3$ are a Seyfert 2 and a starbursting S0 galaxy.

Our conclusion, then, is that all non-central-dominant early-type galaxies within our sample, apart from a handful which are clearly peculiar, populate a band in L_X/L_B which lies between the discrete source contribution and the expected luminosity from discrete sources plus a cooling halo of gas released from galactic stars. This band covers a range of L_X/L_B which changes only weakly with L_B (the lower bound in Figure 8 is horizontal, whilst the upper bound rises by only a factor ~ 3 over the range $L_B = 10^9 - 10^{11} L_{\odot}$), and where we have reasonable data, our galaxies appear to populate the whole band. It is therefore not surprising that the mean L_X/L_B ratio shows no significant trend with L_B . Larger samples of galaxies would be required to convincingly resolve any trend associated with the upper boundary of the band.

The fact that group galaxies (at least in the range $L_B = 10^{10} - 11^{10} L_{\odot}$, where we have good coverage) span the full range from discrete source to full cooling halo lines, indicates that their hot halos cover a wide range of states. The most X-ray underluminous systems have either lost all their gas as a result of some recent stripping or star formation event, or are in a wind phase, in which most of the gas lost by stars streams out of the galaxy in a fast, low-density wind (Ciotti et al. 1991). There is an interesting indication from Figure 5, that such systems are not represented amongst our sample of genuinely isolated early-type galaxies, though better statistics are required to be sure. If confirmed, this observation may relate to the low inci-

dence of tidal interaction and interaction-induced starburst activity expected in isolated galaxies, compared to those in groups. Galaxies with intermediate L_X/L_B values may be in ‘partial wind’ stages (Pellegrini & Ciotti 1998), and high resolution X-ray studies with Chandra and XMM-Newton can be used to search for central cooling flows within such systems. The non-central-dominant galaxies with the highest values of L_X/L_B are likely to have hot hydrostatic halos with fully developed galactic cooling flows. However unlike central dominant galaxies, we see no evidence that these non-central galaxies have excess X-ray luminosity due to accretion of external gas from the group. Presumably their motion prevents this.

Turning finally to the the central-dominant group galaxies – these mostly fall above the upper boundary marked in Figure 8. Gas loss from within the galaxy is unable to explain the high luminosity and temperature, and the large extent of the X-ray emission in these galaxies, as pointed out by Brighenti & Mathews (1999) and Brown & Bregman (2000). It appears that additional infalling material is required to adequately reproduce their observed properties (Brighenti & Mathews 1998,1999). The most likely origin of this infalling material, for dominant group galaxies, is a group cooling flow, since the X-ray properties of these galaxies appear to be more closely related to the group than to the galaxy itself (Helsdon & Ponman 2001).

If this picture is correct, the most X-ray over-luminous early-type galaxies should be found in the centres of undisturbed bright groups and clusters. Other early-type galaxies within galaxy systems should have much lower values of L_X/L_B , unless of course they have been the central galaxy of a group which has recently merged with the present cluster. In addition, disturbed clusters which show no evidence of any cooling flow would be expected to contain central galaxies that are less X-ray over-luminous than clusters and groups with cooling flows.

If central group galaxy X-ray properties are more strongly related to the group than to the galaxy this would account for some of the scatter in the early-type galaxy L_X/L_B relation. It would also explain the correlation of X-ray luminosity with the relative sizes of the X-ray and optical emission found by Mathews & Brighenti (1998): the most X-ray over-luminous galaxies should be found in the centre of bigger groups. In addition, the apparent lack of rotationally enhanced X-ray ellipticity in the cooling flows of elliptical galaxies (Hanlan & Bregman 2000), may be explained if it is a group, rather than galaxy cooling flow.

8 CONCLUSIONS

We have derived the X-ray luminosity for a sample of galaxies in groups after allowing for the effects of the intragroup emission. This sample is used to derive the $L_X:L_B$ relation for both early- and late-type galaxies in groups, and these relations are compared to those derived for other environments.

In general, the X-ray properties of spiral galaxies appear to be indistinguishable from those in other environments. We find no significant deviations from the $L_X:L_B$ and $L_X:L_{FIR}$ relations of spirals derived from more general samples.

The X-ray properties of early-type galaxies appear to fall into two distinct categories – central-dominant group galaxies, and non-central-dominant galaxies. The non-central group galaxies populate a band in L_X/L_B which shows no discernible trend with optical luminosity in our data, and is well explained by a combination of emission from discrete galactic X-ray sources together with a variable contribution from hot gas released by stars. In contrast the central-dominant group galaxies are far more X-ray luminous. In the region where the optical luminosity of the central galaxies overlaps with the non-central sample their X-ray luminosity is over an order of magnitude greater. It appears that infall of gas from the intragroup medium is required to account for these large luminosities.

We have compared the properties of the early-type galaxies in groups with those in other environments by deriving X-ray luminosities for a sample of isolated galaxies and also by splitting previous large surveys of early-type galaxies into group and field subsamples. Non-central-dominant galaxies in groups have a $L_X:L_B$ relation of slope unity, and the resulting mean value of L_X/L_B appears essentially identical for isolated and group galaxies. We suggest that steeper $L_X:L_B$ slopes derived in previous work, and apparent dependence of L_X/L_B on surrounding galaxy density, result from the inclusion of central-dominant group galaxies in galaxy samples.

9 ACKNOWLEDGEMENTS

The authors would like to thank Craig Sarazin for providing pre-publication information on the spectral characteristics of discrete source populations in early-type galaxies, and to acknowledge useful discussions with Joel Bregman and Bill Mathews. We would also like to thank the referee, Jimmy Irwin, for suggesting several improvements to the paper. The data used in this work have been obtained from the Leicester database and archive service (LEDAS). This work made use of the Starlink facilities at Birmingham and the NASA/IPAC Extragalactic Database (NED). SFH acknowledges financial support from the University of Birmingham and EJOS acknowledges the receipt of a PPARC studentship.

REFERENCES

- Abell G. O., Corwin H. G. J., Olowin R. P., 1989, ApJS, 70, 1
- Amendola L., Di Nella H., Montuori M., Sylos Labini F., 1997, Fractals, 5, 635
- Beuing J., Dobreiner S., Böhringer H., Bender R., 1999, MNRAS, 302, 209
- Blanton E. L., Sarazin C. L., Irwin J. A., 2000, ApJ, in press
- Boller T., Meurs E. J. A., Brinkmann W., Fink H., Zimmerman U., Adorf H.-M., 1992, A&A, 261, 57
- Bothun G. D., Lonsdale C. J., Rice W., 1989, ApJ, 341, 129

- Brighenti F., Mathews W. G., 1998, *ApJ*, 495, 239
- Brighenti F., Mathews W. G., 1999, *ApJ*, 512, 65
- Brown B. A., Bregman J. N., 1998, *ApJ*, 495, L75
- Brown B. A., Bregman J. N., 2000, *ApJ*, 539, 592
- Canizares C. R., Stewart G. C., Fabian A. C., 1983, *ApJ*, 272, 449
- Canizares C. R., Fabbiano G., Trinchieri G., 1987, *ApJ*, 312, 503
- Cappellaro E., Evans R., Turatto M., 1999, *A&A*, 351, 459
- Ciotti L., Pellegrini S., Renzini A., D'Ercole A., 1991, *ApJ*, 376, 380
- Davis D. S., White R. E. I., 1996, *ApJ*, 470, L35
- Devereux N. A., Eales S. A., 1989, *ApJ*, 340, 708
- Eskridge P. B., Fabbiano G., Kim D.-W., 1995, *ApJS*, 97, 141
- Fabbiano G., Trinchieri G., 1985, *ApJ*, 296, 430
- Fabbiano G., Gioia I. M., Trinchieri G., 1988, *ApJ*, 324, 749
- Faber S. M., Wegner G., Burstein D., L. D. R., Dressler A., Lynden-Bell D., Terlevich R. J., 1989, *ApJS*, 69, 763
- Forbes D. A., 1992, *A&AS*, 92, 583
- Forman D., Jones C., Tucker W., 1985, *ApJ*, 293, 102
- Garcia A. M., 1993, *A&AS*, 100, 47
- Gunn J. E., Gott J. R., 1972, *ApJ*, 176, 1
- Hanlan P. C., Bregman J. N., 2000, *ApJ*, 530, 213
- Hau G. K. T., Carter D., Balcells M., 1999, *MNRAS*, 306, 437
- Helsdon S. F., Ponman T. J., 2000, *MNRAS*, 315, 356
- Helsdon S. F., Ponman T. J., 2001, in prep.
- Hickson P., Kindl E., Auman J. R., 1989, *ApJS*, 70, 687
- Hickson P., 1982, *ApJ*, 255, 382
- Hickson P., 1997, *ARA&A*, 35, 357
- Irwin J. A., Sarazin C. L., 1998, *ApJ*, 499, 650
- Kim D.-W., Fabbiano G., Trinchieri G., 1992, *ApJ*, 393, 134
- Mathews W. G., Brighenti F., 1998, *ApJ*, 493, L9
- Matsumoto H., Koyama K., Awaki H., Tsuru T., Loewenstein M., Matsushita K., 1997, *ApJ*, 482, 133
- Matsushita K., Ohashi T., Makishima K., 2000, *PASJ*, 52, 685
- Mendes de Oliveira C., Hickson P., 1994, *ApJ*, 427, 684
- Mulchaey J. S., Zabludoff A. I., 1999, *ApJ*, 514, 133
- Mulchaey J. S., Davis D. S., Mushotzky R. F., Burstein D., 1996, *ApJ*, 456, 80
- Nulsen P. E. J., 1982, *MNRAS*, 198, 1007
- Okamoto T., Habe A., 1999, *ApJ*, 516, 591
- O'Sullivan E., Forbes D. A., Ponman T. J., 2000, in prep
- Pellegrini S., Ciotti L., 1998, *A&A*, 333, 433
- Pietsch W., Trinchieri G., Arp H., Sulentic J. W., 1997, *A&A*, 322, 89
- Ponman T. J., Allan D. J., Jones L. R., Merrifield M., McHardy I. M., Lehto H. J., Luppino G. A., 1994, *Nature*, 369, 462
- Ponman T. J., Bourner P. D. J., Ebeling H., Böhringer H., 1996, *MNRAS*, 283, 690
- Prugniel P., Simien F., 1996, *A&A*, 309, 749
- Raymond J. C., Smith B. W., 1977, *ApJS*, 35, 419
- Read A. M., Ponman T. J., 1998, *MNRAS*, 297, 143
- Read A. M., Ponman T. J., 2001, in prep.
- Rubin V. C., Hunter D. A., Ford W. K. J., 1991, *ApJS*, 76, 153
- Sansom A. E., Reid I. N., C. B., 1988, *MNRAS*, 234, 247
- Sarazin C. L., Irwin J. A., Bregman J. N., 2000, *ApJ*, 544, L101
- Schindler S., Binggeli B., Bhringer H., 1999, *A&A*, 343, 420
- Shapley A., Fabbiano G., Eskridge P. B., 2000, preprint
- Shimada M., Ohyama Y., Nishiura S., Murayama T., Taniguchi Y., 2000, *AJ*, 119, 2664
- Stark A. A., Gammie C. F., Wilson R. W., Bally J., Linke R. A., Heiles C., Hurwitz M., 1992, *ApJS*, 79, 77
- Trinchieri G., Fabbiano G., 1985, *ApJ*, 296, 447
- Tully R. B., 1987, *ApJ*, 321, 280
- Tully R. B., 1988, *Nearby Galaxies Catalog*. Cambridge University Press
- Verdes-Montenegro L., Yun M. S., Williams B. A., Huchtmeier W. K., Del Olmo A., Perea J., 2000, in Valtonen M., Flynn C., eds, *ASP Conf. Ser. 209: Small Galaxy Groups*. p. 167
- Vikhlinin A., McNamara B. R., Hornstrup A., Quintana H., Forman W., Jones C., Way M., 1999, *ApJ*, 520, L1
- White R. E. I., Sarazin C. L., 1991, *ApJ*, 367, 476

Zabludoff A. I., Mulchaey J. S., 1998, *ApJ*, 496, 39

Zepf S. E., Whitmore B. C., 1993, *ApJ*, 383, 542